The magnetization distributions in some Heusler alloys proposed as half-metallic ferromagnets

2000 J. Phys.: Condens. Matter 12 1827

(http://iopscience.iop.org/0953-8984/12/8/325)

J. Phys.: Condens. Matter **12** (2000) 1827–1835. Printed in the UK PII: S0953-8984(00)09245-6

The magnetization distributions in some Heusler alloys proposed as half-metallic ferromagnets

P J Brown†‡, K U Neumann†, P J Webster§ and K R A Ziebeck†

† Department of Physics, Loughborough University, Loughborough, Leics LE11 3TU, UK
‡ Institut Laue–Langevin, BP 156, 38042 Grenoble Cédex, France
§ Department of Civil Engineering, University of Salford, Salford M5 4WT, UK

Received 3 November 1999

Abstract. The magnetization distributions in a series of ternary intermetallic compounds based on the composition Co_2YZ where Y is Ti, Mn or Fe and Z a subgroup-B element have been determined from polarized neutron diffraction measurements. Comparison of the magnetic structure factors with model calculations shows that the magnetization is associated principally with those atoms which in their elemental state are themselves magnetic. The observed deviations of the magnetic moment distributions from spherical symmetry have been used to deduce which of the 3d sub-bands are active at the Fermi energy. A small moment close to the limits of resolution is observed at some of the Z sites, together with a small delocalized moment which in most cases is negative. The results have been compared with the predictions of band models, which indicate that the Fermi level falls in a broad minimum in the minority-spin density of d states. Although the identity of the bands active at the Fermi surface is in broad agreement with predictions of band-structure calculations (Ishida S, Akazawa S, Kubo Y and Ishida J 1982 *J. Phys. F: Met. Phys.* **12** 1111), the results suggest that there is a finite density of states in the minority-spin d band of manganese. Hence the compounds cannot be classified as half-metallic ferromagnets.

1. Introduction

There are a large number of ferromagnetic ternary intermetallic compounds which adopt the Heusler alloy structure ($L2_1$). Ideally these alloys have composition X_2YZ. In general X and Y are transition metals and Z is a B-subgroup element. For some time, interest was focused on systems in which the magnetic moment is confined to manganese atoms occupying the Y position. These are good model systems for studying localized 3d metallic magnetism since there is negligible overlap between the Mn 3d wave functions. In these systems the 3d electrons, which give nearly the full moment of 5 μ_B, do not participate in the Fermi surface. The situation is somewhat modified when the X atom is one which in its elemental state is strongly ferromagnetic such as Fe or Co. The unfilled d shells of these atoms overlap with those of their manganese neighbours, so direct exchange becomes possible. Magnetization and neutron diffraction measurements have revealed that all known Heusler alloys in the Co_2MnZ series are ferromagnetic with a significant moment on the Co as well as on the Mn sites. The alloys in this series all have relatively high Curie temperatures when compared with most other Heusler alloys. In particular, the Curie temperature 985 K of Co_2MnSi is the highest among those of all known Heusler alloys containing manganese [2].

Recently there has been an upsurge of interest in these alloys triggered by the possibility that they are *half-metallic ferromagnets*. Half-metallic ferromagnets are systems in which at the Fermi level the density of states of one spin sub-band is very small whereas that of the other

0953-8984/00/081827+09$30.00

is large. Such systems have metallic behaviour for electrons of one spin state and insulating behaviour for the other. The interest [3, 4] in half-metallic ferromagnets stems from their potential for technological applications particularly in the area of spin electronics, e.g. spin valves. The absence of spin-down states at E_F can also modify the thermal variation of the resistivity at low temperature. Half-metallic ferromagnets were first predicted [5] to occur in intermetallic compounds containing manganese, with the semi-Heusler cubic $C1_b$ structure, such as NiMnSb. More recent band-structure calculations have predicted similar properties for related iron- and cobalt-based Heusler alloys [6], CrO_2 [7, 8] and doped manganese perovskites [9]. Complete spin polarization of the 3d band in half-metallic ferromagnets should be evident in spin-resolved photoemission. However, such measurements [10] on NiMnSb only revealed 50% polarization. In CrO_2, 100% spin polarization was observed [11] but at a binding energy of 2 eV rather than at E_F where almost no spectral weight appears for either spin direction. Similar measurements [3] on $La_{0.7}Sr_{0.3}MnO_3$ indicate a Fermi cut-off for the majority-spin band whereas the minority-spin band exhibits an insulating gap with the spectral weight disappearing at a binding energy of $\sim$0.6 eV. Polarized neutron diffraction provides an alternative and more stringent means of testing the predictions of band theory by measurement of the spatial distribution of the magnetization. To date such measurements on possible half-metallic magnets have only been reported for NiMnSb [12] and Fe_2MnSi [13]. The former compound has a non-centro-symmetric space group which complicates the analysis, but the results for Fe_2MnSi suggest that it approximates closely to a half-metallic ferromagnet as is also suggested by band theory [6].

Half-metallic behaviour has also been predicted [6] for Co_2MnSi, which is a member of the series of ferromagnetic Heusler alloys in which both the cobalt and manganese atoms carry moments. It is well established that the magnetic properties of these compounds depend sensitively on the degree of atomic order and on the conduction electron concentration [14]. The magnetic properties depend [2] on whether the Z component comes from the 3B or 4B subgroup, with the latter group having higher magnetic moments and Curie temperatures. Spin-polarized band-structure calculations [1, 15, 16] indicate that the moments are predominantly of 3d origin and that the shapes of the densities of states for Co and Mn are similar. The DOS of the minority band is almost zero at E_F whereas the majority d band has a small peak near to this energy. It is the filling or emptying of this peak that is assumed to produce the change in moment size and Curie temperature as the Z component changes. In order to test this hypothesis, and to obtain further evidence for half-metallic behaviour, we have made polarized neutron diffraction measurements on a series of Co_2MnZ compounds and on two related compounds in which Mn is replaced first by a ferromagnetic atom (Co_2FeGa) and then by a non-magnetic one (Co_2TiSn).

2. Experimental details

2.1. Sample preparation

Ingots of Co_2MnZ (Z = Si, Ga, Ge and Sn) and of Co_2FeGa and Co_2TiSn were grown from starting materials of 5N purity, using the Bridgman technique, by Perrier de la Batthie at CNRS, Grenoble. The ingots were examined using the Laue neutron diffraction technique. Single crystals were cut from each ingot in the form of rectangular parallelepipeds with approximate dimensions 1.5 × 1.5 × 5.0 mm. The long axis coincided approximately with a ⟨110⟩ zone axis. All of the compounds order in the Heusler $L2_1$ structure, details of which are given in table 1.

Table 1. Crystallographic data for Heusler alloys.

Space group $Fm3m$		
Site	Atomic positions	
A (Mn, Fe, Ti)	4a	000
B (Si, Ga, Ge, Sn)	4b	$\frac{1}{2}\frac{1}{2}\frac{1}{2}$
C (Co)	8c	$\frac{1}{4}\frac{1}{4}\frac{1}{4}$

2.2. Bulk magnetization measurements

Bulk magnetization measurements were made using a vibrating-sample magnetometer in fields up to 1.6 T and at stable temperatures between 4 and 300 K. The samples used were cut from the same ingots as the single crystals used in the neutron experiments. The results, which are summarized in table 2, were, within the accuracy of the measurements, identical to those obtained earlier on polycrystalline samples [2, 17].

Table 2. Summary of bulk properties.

	a (Å)	σ_{0T} (emu g^{-1})	σ_{0T} (μ_B/f.u.)	T_c (K)
Co_2MnSi	5.654	138.0	4.96	985
Co_2MnGa	5.770	86.0	3.72	694
Co_2MnGe	5.743	111.75	4.84	905
Co_2MnSn	6.000	91.5	4.78	829
Co_2TiSn	6.073	36.25	1.85	359
Co_2FeGa	5.737	118.6	5.15	>1100

2.3. Neutron diffraction measurements

The crystals were mounted with their long axes vertical on a cadmium-tipped soft iron pin, which was then fixed in a special jig containing soft iron pole-pieces. The assembly was located at the centre of an electromagnet on the D3 polarized neutron diffractometer at the ILL, Grenoble. The electromagnet had a truncated cone pole-piece that had been bored axially to permit vertical insertion of the specimen assembly, and provided a uniform vertical magnetic field of 1.5 T at the sample position. The diffractometer was operated in the normal beam mode; the range of angles by which the detector could be tilted out of the horizontal plane was -8° to $+35^\circ$. Polarization ratio measurements were made, using a wavelength of 0.9 Å, for all reflections (hkl) in the zero and first layers for values of $(\sin\theta)/\lambda \leqslant 0.75$ Å^{-1}. Since the Curie temperatures of the Co_2MnZ series are so high, all measurements on these compounds were made at room temperature. For Co_2FeGa which has a Curie temperature in excess of 1100 K the measurements were made at 223 K, but for Co_2TiSn which has a considerably lower ordering temperature the measurements were carried out at 100 K with the sample magnetized using a superconducting magnet producing a field of 4.6 T. The degree of polarization of the incident beams, and the depolarization due to the crystals, were determined using standard CoFe and Cu_2MnAl crystals as described by [18]. To check for the presence of extinction and to ascertain the degree of atomic order, measurements of the integrated intensities were made using the same samples on the D9 single-crystal diffractometer at the ILL. Over 250 separate reflections were measured for each crystal at two wavelengths, 0.84 and 0.5 Å.

3. Refinement of the nuclear structure

The integrated intensity data measured on D9 were corrected for the Lorentz factor and the intensities of ≈60 independent reflections were derived for each compound at each of the two wavelengths. Each reflection intensity was obtained from the mean of measurements made on several equivalents. The nuclear structure factors were derived from these intensities by subtracting the magnetic contributions indicated by the measured polarization ratios. In all the measurements, apart from those on Co_2FeGa, no significant differences were observed, after scaling, between the two data sets obtained using different wavelengths, indicating that extinction effects were negligible in these crystals. The nuclear scattering lengths and isotropic temperature factors for the three sites in each compound were obtained from least-squares refinements. For Co_2FeGa a single extinction parameter to model the mosaic spread in the Becker–Coppens formalism [19] was also included in the refinement. The results are shown in table 3. For normalization purposes the sum of the site scattering lengths $b_A + b_B + 2b_C$ was fixed to accord with the stoichiometric composition. From table 3 it may be seen that all of the crystals were highly ordered in the Heusler $L2_1$ structure. There is evidence for a small degree of disorder (≈4%) between the A and B sites in Co_2MnGa and Co_2MnGe, whereas in Co_2TiSn the relatively high values obtained for the scattering lengths of the A and B sites suggest a small deficit (≈5%) in the C-site occupancy. For Co_2FeGa the neutron data do not define the site occupancies with such good precision because of lower contrast between the atomic scattering lengths.

Table 3. Site parameters of the least-squares structural refinement of Co_2YZ compounds.

Scattering lengths (fm)							
Co: 2.50	Mn: −3.73	Si: 4.15	Ga: 7.29	Fe: 9.54	Ti: −3.30	Ge: 8.19	Sn: 6.23
	Sites						
	C		A		B		
	b (fm)	B (Å^{-2})	b (fm)	B (Å^{-2})	b (fm)	B (Å^{-2})	R (%)[a]
Co_2MnSi	2.45(1)	0.302(6)	−3.62(2)	0.293(6)	4.13(2)	0.338(6)	1.1
Co_2MnGa	2.42(4)	0.315(11)	−3.31(3)	0.299(12)	7.07(6)	0.347(6)	1.3
Co_2MnGe	2.59(4)	0.37(2)	−3.25(4)	0.307(17)	7.52 (6)	0.388(8)	1.5
Co_2MnSn	2.55(2)	0.64(8)	−3.66(4)	0.53(7)	6.21(4)	0.60(5)	3.3
Co_2TiSn	2.55(2)	0.209(12)	−3.65(2)	0.233(11)	6.45(2)	0.211(6)	2.4
Co_2FeGa	2.7(3)	0.32(5)	9.0(5)	0.32(5)	7.5(5)	0.37(1)	1.6

[a] Crystallographic R-factor: $\sum |F_{obs} - F_{calc}| / \sum F_{obs}$.

4. Analysis of the polarized neutron data

The ratios of the magnetic to the nuclear structure factors were calculated from the observed polarization ratios, making appropriate corrections for depolarization, flipper efficiency and the inclination of the scattering vector to the polarization direction. These ratios were multiplied by nuclear structure factors, calculated using the parameters obtained in the refinement described above, to obtain the magnetic structure factors. Each magnetic structure factor was the mean of several measurements of each of a number of equivalent reflections. In almost all cases the difference between measurements of equivalent reflections was not statistically significant.

4.1. Models of the magnetization

A preliminary determination of the magnetic moments associated with the different sites was made by associating a spherically symmetric Co^{2+} form factor with the C sites and a spherically symmetric Mn^{2+} or Fe^{2+} form factor with the A sites. The form factors used were those calculated for the free ions [20]. A least-squares determination of the moment values from the magnetic structure factors gave results which are shown in table 4; the R-values corresponding to the fits are also shown in the table.

Table 4. Magnetic moment and form factor parameters obtained from different least-squares fits to the magnetic structure factors of Co_2YZ alloys.

	Site								
	C			A			B		
Alloy	a_0[a]	a_2	a_4	a_0	a_2	a_4	a_0	a_2	R (%)
Co_2MnSi	1.16(3)	−0.05(3)	0.26(3)	3.34(5)	−0.16(5)	0.50(5)			6
	1.20(3)	−0.09(3)	0.27(3)	3.35(4)	−0.17(4)	0.55(4)	0.17(4)[b]	−0.16(4)	4
	1.20(3)	−0.09(3)	0.26(5)	3.37(5)	−0.20(5)	0.50(5)	0.2(3)[c]	0.4(3)	5
Co_2MnGa	1.00(3)	−0.15(6)	0.28(5)	2.75(4)	0.32(9)	0.32(7)			6
	0.97(2)	−0.01(4)	0.28(3)	2.75(2)	0.34(6)	0.32(5)	−0.14(2)[b]	0.05(2)	4
Co_2MnGe	0.72(4)	0.31(9)	0.28(7)	3.07(5)	0.24(8)	0.38(9)			8
Co_2MnSn	0.85(3)			3.28(5)			0.09(5)[b]		10
	0.87(4)	0.02(5)	0.29(5)	3.29(5)	0.17(5)	0.14(5)	0.09(3)[b]		5
Co_2TiSn	1.05(3)			0.07(6)			0.04(4)[d]		27
	1.05(3)	−0.06(7)	0.43(7)	0.01(3)	0.27(6)		0.08(2)[d]		17
Co_2FeGa	1.15(4)			2.47(5)			0.29(5)[b]		14
	1.06(3)	0.11(3)	0.25(3)	2.38(4)	0.12(5)	0.30(5)	0.22(3)[b]		6

[a] The values of a_0, a_2 and a_4 are given in μ_B.
[b] With the A-site form factor.
[c] With the Si 3p form factor.
[d] With the Co 3d form factor.

The goodness of fit of the spherical model was assessed by calculating

$$\chi^2 = \sum [(F_{obs} - F_{calc})/\sigma F_{obs}]^2/(N_{obs} - N_{pars})$$

where N_{obs} is the number of observations and N_{pars} the number of fitted parameters. The values obtained were much greater than unity which shows that the model is too restrictive. A slightly more sophisticated model was therefore employed in which the magnetic scattering from each site is given by

$$F_a(\boldsymbol{k}) = a_0\langle j_0(k)\rangle + a_2\langle j_2(k)\rangle + a_4 A(\boldsymbol{k})\langle j_4(k)\rangle$$

$$\langle j_l(k)\rangle = \int_0^\infty J_l(kr)U^2(r)\,\mathrm{d}r^3$$

and

$$A(k) = \frac{3(h^4 + k^4 + l^4) - 9(h^2k^2 + k^2l^2 + l^2h^2)}{(h^2 + k^2 + l^2)^2}.$$

$J_l(kr)$ is an lth-order spherical Bessel function and $U^2(r)$ is the radial distribution function of the magnetic electrons. In this formulation the coefficient a_0 is the atomic magnetic moment, a positive coefficient a_2 describes an expansion of the form factor, possibly due to the orbital magnetic moment, and the coefficient a_4 measures the degree of asphericity of the moment

distribution. In the dipole approximation the spectroscopic splitting factor g is given by $g = 2/(1-a_2)$. The fraction of the magnetic electrons in e_g orbitals γ is $\frac{2}{5}(3a_4/a_0+1)$. In the first instance the radial wave functions used were those calculated for the Co^{2+} $3d^74s^0$ (5D), Fe^{2+} $3d^64s^0$ (5D) and Mn^{2+} $3d^54s^0$ (6S) configurations [21] on the C and A sites respectively. The magnetic moments and the values of the parameters obtained from a least-squares fit of the magnetic structure factors to this model are compared with those for the spherical models in table 4, together with their corresponding R-factors. The effect on the parameters and on the goodness of fit of changing the radial distribution functions into those corresponding to neutral atoms, and of mixing the radial functions of cobalt and manganese on the two sites in the proportions corresponding to the degree of order was investigated. Changing the radial distribution functions has only a very small effect on the values of the parameters, and does not improve the goodness of fit. The models in which the transition metal d electrons have form factors corresponding to neutral-atom wave functions give marginally better fits than those in which the form factors are for ionized states. Most importantly, the minimum values of χ^2 obtained were still significantly greater than unity, indicating that there remain very significant differences between the actual observations and the predictions of the model. Two further types of model calculation were carried out in both of which a moment was allowed to reside on the B site. In one calculation it was assumed that the moment was associated with transition metal atoms at the B sites and in the other that the moment was associated with the Z atom itself. It was found that for some of the alloys allowing such a moment gave a better fit. The refinements show that its form factor falls off more rapidly than that of Mn^{2+} but less rapidly than that of the p electrons of the corresponding Z atom. This can be seen in the results given for Co_2MnSi in table 4 where the a_2-coefficient is negative, giving a contraction, when the Mn 3d form factor is used; and positive, giving an expansion, if the moment is associated with the Si 3p form factor. It should be emphasized that the models that we have used to fit the data are quite restrictive, hence the relatively large residuals. The fit is particularly poor for Co_2TiSn because all of the hkl odd reflections (about half of all those measured) have very little magnetic scattering as they have no contribution from the spherical part of the Co moment. They are thus particularly sensitive to defects of the model.

5. Discussion

The spin and orbital magnetic moments associated with the C and A sites are given in table 5. They have been obtained by assuming that the expansion of the form factor, associated with the parameter a_2 in the model, is due to the orbital moment. The magnetic moments associated

Table 5. Magnetic moments in cobalt-based Heusler alloys.

	C sites		A sites		B sites	Total per f.u.	
Alloy	μ_S (μ_B)	μ_L (μ_B)	μ_S (μ_B)	μ_L (μ_B)	μ (μ_B)	μ_s (μ_B)[a]	μ_m (μ_B)[b]
Co_2MnSi	1.29(4)	−0.09(3)	3.52(5)	−0.17(4)	0.17(4)	5.92(8)	4.96
Co_2MnGa	0.98(4)	−0.01(4)	2.41(6)	0.34(6)	−0.14(2)	4.55(6)	3.72
Co_2MnGe	0.41(9)	0.31(9)	2.83(10)	0.24(8)		4.51(8)	4.84
Co_2MnSn	0.85(6)	0.02(5)	3.12(7)	0.09(3)	0.09(3)	5.12(8)	4.78
Co_2TiSn	1.11(8)	−0.06(7)	−0.26(8)	0.27(6)	0.08(2)	2.19(7)	1.85
Co_2FeGa	0.95(4)	0.11(3)	2.26(6)	0.12(5)	0.22(3)	4.72(8)	5.15

[a] Magnetic moment from diffraction measurements.
[b] Magnetic moment from saturation magnetization.

with the B sites and the total magnetic moment per formula unit obtained from the neutron diffraction data are also listed in the table as are the magnetic moments per formula unit obtained from the saturation magnetization. In general the expansion of the form factor which has been modelled using $\langle j_2 \rangle$ is small, and the values for Co are not incompatible with the orbital moment in Co_2MnSn and Co_2TiSn calculated by [22]. The experimental value obtained for Co_2MnGe is anomalous. For Mn there is a significant expansion of the form factor in both the Ge and Ga compounds. The Ti moment in Co_2TiSn is probably induced by the internal field; the spin and orbital contributions are opposite and nearly equal. For all of the alloys except Co_2MnGe and Co_2FeGa the sum of the atomic moments is greater than that expected from the saturation magnetization measurements. This may be due to the presence of a negative diffuse moment amounting to some 0.15 μ_B Å^{-3}.

The degree of asymmetry given by the a_4-parameters has been used to calculate the numbers of magnetic carriers associated with the A and C sites which have e_g and t_{2g} symmetries. These are compared with the values obtained for related alloys in table 6.

Table 6. Magnetic moments and symmetries associated with the different atomic sites in X_2YZ compounds. The moments μ are given in μ_B and γ is the fraction of the magnetic carriers with e_g symmetry. Data for Fe_3Si and Fe_4Si are taken from reference [23], for Fe_3Al from reference [24] and for Fe_2MnSi from reference [13].

	C sites				A sites			
			No of carriers				No of carriers	
Alloys	μ	γ	e_g	t_{2g}	μ	γ	e_g	t_{2g}
Co_2MnSi	1.20	0.72	0.86	0.34	3.37	0.46	1.55	1.92
Co_2MnGa	0.97	0.75	0.73	0.24	3.01	0.54	1.62	1.38
Co_2MnGe	0.72	0.86	0.62	0.10	3.07	0.55	1.67	1.38
Co_2MnSn	0.87	0.80	0.70	0.17	3.29	0.45	1.48	1.81
Co_2TiSn	1.05	0.89	0.93	0.12				
Co_2FeGa	1.06	0.68	0.72	0.34	2.56	0.55	1.46	1.10
Fe_2MnSi	0.32	0.66	0.28	0.04	1.62	0.59	0.96	0.66
Fe_3Si	1.07	0.77	0.59	0.48	2.23	0.58	1.29	0.94
Fe_4Si	1.31	0.82	0.75	0.56	2.33	0.58	1.35	0.98
Fe_3Al	1.5	0.8	0.76	0.82	2.18	0.60	1.31	0.87

In general the C site (Co) always has a large preponderance of e_g carriers. Within the Co_2MnX series, the larger the Co moment, the smaller the γ-value. When the moment increases the number of both kinds of carrier goes up. It is reasonable to assume that within the Co_2MnZ series the basic shape of the density of states (DOS) corresponding to the Co and Mn electrons remains the same; changing the Z element will cause the effective position of the Fermi surface (FS) to change, either due to changes in the effective e/a, or details of shape depending on interatomic distances and electrostatic potentials. The change in the number of carriers with changing Z shows that the DOS at E_F must be almost the same in the t_{2g} and e_g sub-bands. For the A (Mn/Fe) sites the number of carriers of e_g symmetry varies rather little whilst that of carriers of t_{2g} symmetry varies much more. Moreover an increasing magnetic moment is associated with a decrease in the number of e_g carriers and an increase in the number of t_{2g} ones. This suggests that for Mn the majority-spin t_{2g} sub-band must have a relatively high DOS at E_F and that the higher DOS in the e_g band at E_F occurs in the minority band.

Figure 1 shows a rough sketch of the DOS calculated for both the Co and Mn d electrons in Co_2MnSn by [1]. Both are characterized by the very low DOS predicted for the minority spins. The DOS is higher in the majority-spin band and for the cobalt site has almost equal

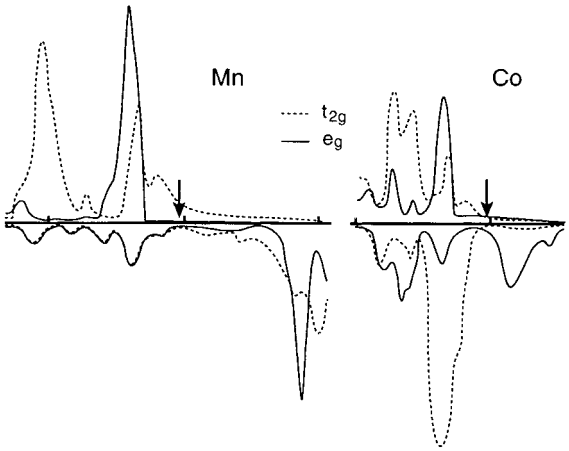

Figure 1. A sketch of the DOS calculated for the Co and Mn 3d electrons in Co_2MnSn [1]. The top curves show the DOS of the majority spins and the lower curves those of the minority spins. The dashed lines correspond to states with t_{2g} symmetry and full ones to states with e_g symmetry. The Fermi energy is indicated by the bold arrows.

contributions from e_g and t_{2g} electrons which accords with the polarized neutron measurements. However, the small peak in the DOS which lies just below E_F has a much higher DOS of t_{2g} than of e_g electrons and can therefore not account for the changing moment in the range of alloys studied.

For Mn the majority e_g band is nearly full and has a low DOS at E_F, the higher DOS being in the t_{2g} band again in accordance with our measurements. However, there does not seem to be a high enough DOS in the minority-spin e_g band at E_F to account for the observed diminution in the number of e_g carriers with increasing moment. The Co site of the Co_2TiSn alloy in which Mn is replaced by Ti shows the highest percentage of e_g electrons of all the compounds measured. This is not expected from the band-structure calculations [1] in which the principal difference in the Co DOS between Co_2TiSn and Co_2MnSn is that the former has a significant value in the minority-spin e_g band at E_F whereas for the latter it is nearly zero. This should lead to a smaller rather than a larger percentage of e_g carriers. There are no band-structure calculations available for Co_2FeGa; however, the symmetries of the magnetization at the A and C sites are very similar to those found for the cobalt–manganese series, suggesting a similar DOS. Indeed there is rather little change in the symmetries of these two sites over the whole range of alloys shown in table 6, showing that these are more closely linked to the identity of the sites, rather than to the actual atoms occupying them.

In conclusion, there is rather good agreement between the polarized neutron results and the band-structure calculations for the Co sites in the alloys containing manganese, and the cobalt DOS exhibits half-metallic ferromagnetism. On the other hand our results seem to require a finite density of states in the minority-spin band of manganese, so these alloys cannot be classified as true half-metallic ferromagnets.

Acknowledgments

We would like to thank M Mankikar for help with the experiments and for making the magnetization measurements. We are grateful to Professor S Ishida for providing unpublished details of his band-structure calculations.

References

[1] Ishida S, Akazawa S, Kubo Y and Ishida J 1982 *J. Phys. F: Met. Phys.* **12** 1111
[2] Webster P J 1971 *J. Phys. Chem. Solids* **32** 1221
[3] Park J-H, Vescovo E, Kim H-J, Kwon C, Ramesh R and Venkatesan T 1998 *Nature* **392** 794
[4] Pickett W E 1998 *Phys. World* **11** (7) 22
[5] de Groot R A, Muller F M, van Engen P G and Buschow K H J 1983 *Phys. Rev. Lett.* **50** 2024
[6] Fujii S, Ishida S and Asano S 1995 *J. Phys. Soc. Japan* **64** 185
[7] Schwarz K 1986 *J. Phys. F: Met. Phys.* **16** L211
[8] Lewis S P, Allen P B and Saski T 1997 *Phys. Rev.* B **55** 10 253
[9] Pickett W E and Singh D J 1997 *J. Magn. Magn. Mater.* **172** 237
[10] Bona G L, Meier F, Taborelli M, Bucher E and Schmidt P H 1985 *Solid State Commun.* **56** 391
[11] Kämper K P, Schmitt W, Güntherodt G, Gambin R J and Ruf R 1988 *Phys. Rev. Lett.* **59** 2788
[12] Hordequin Ch, Lelièvre-Berna E and Pierre J 1997 *Physica* B **234** 602
[13] Brown P J, Ziebeck K R A and Huntley J M 1984 *J. Magn. Magn. Mater.* **50** 169
[14] Jassim I K, Neumann K-U, Visser D, Webster P J and Ziebeck K R A 1992 *J. Magn. Magn. Mater.* **104–107** 2072
[15] Ishida S, Asano S and Ishida J 1984 *J. Phys. Soc. Japan* **53** 2718
[16] Kübler J, Williams A R and Sommers C B 1983 *Phys. Rev.* B **28** 1745
[17] Webster P J and Ziebeck K R A 1973 *J. Phys. Chem. Solids* **34** 1647
[18] Brown P J and Forsyth J B 1964 *Br. J. Appl. Phys.* **15** 1529
[19] Becker P J and Coppens P. 1974 *Acta Crystallogr.* A **30** 139
[20] Watson R E and Freeman A J 1961 *Acta Crystallogr.* **14** 27
[21] Clementi E and Roetti C 1974 *At. Data Nucl. Data Tables* **14** 177
[22] Ishida S, Otsuka Y, Kubo Y and Ishida J 1983 *J. Phys. F: Met. Phys.* **13** 1173
[23] Moss J and Brown P J 1972 *J. Phys. F: Met. Phys.* **2** 358
[24] Pickart S J and Nathans R 1961 *Phys. Rev.* **123** 1163